

****Volume Title****

*ASP Conference Series, Vol. **Volume Number***

****Author****

© ****Copyright Year**** *Astronomical Society of the Pacific*

How SFRIs vary with methods of sampling the IMF and duplicity

John J. Eldridge¹

¹*Institute of Astronomy, University of Cambridge, Madingley Road, Cambridge, CB3 0HA, England.*

Abstract. Using our new Binary Population and Spectral Synthesis (BPASS) code we explore the affect of binary populations on the integrated spectra of galaxies. We also explore the interplay of binary populations and a varying maximum stellar mass. We compare our synthetic populations to observations of $H\alpha$ emission from isolated clusters and $H\alpha$ and FUV observations of galaxies. We find that observations tend to favour a pure stochastic sampling of the initial mass function although the evidence is not significant. We also find that binaries make a stellar population less susceptible to the stochastic effects of filling the IMF. Therefore making it more difficult to determine if there is a variable maximum stellar mass.

1. Introduction

When observations are compared to the results from population synthesis codes perfect agreement is rare. There are many uncertain factors that can be tweaked to achieve a better agreement. The easiest factor to adjust is the initial mass function (IMF). The detail that is never adjusted, beyond altering the metallicity, is the stellar evolution models. This is probably because there are only so many sets of available stellar models for input into population synthesis and each synthesis code has its favourites. More over many stellar evolution groups only provide their *best* models rather than a collection with varying mass-loss, mixing schemes, or binary evolution.

Creating a full set of stellar models was an intensive process requiring a great deal of user and computer time. Today with computer time at a surplus and with recent developments leading to more numerically stable evolution codes it is straight forward to create many different sets of evolution models with varying input physics. This allowed for large numbers of detailed models of binary stars to be created (Eldridge et al. 2008). Therefore we are now able to vary the uncertain details of stellar evolution within our population synthesis code together with other parameters such as the IMF.

Here we discuss how changing between single star to binary models affects the star-formation rate indicators (SFRIs) of $H\alpha$ and the UV luminosity. We also investigate the effect of assuming a varying maximum stellar mass dependent on the star cluster mass on these observables. First we outline our numerical method that uses the recently developed *Binary Population and Spectral Synthesis* (BPASS) code (Eldridge & Stanway 2009). Second we discuss how single stars and binary star populations differ in their predictions for SFRIs when applied to both star clusters and entire galaxies. Finally we summarise our findings.

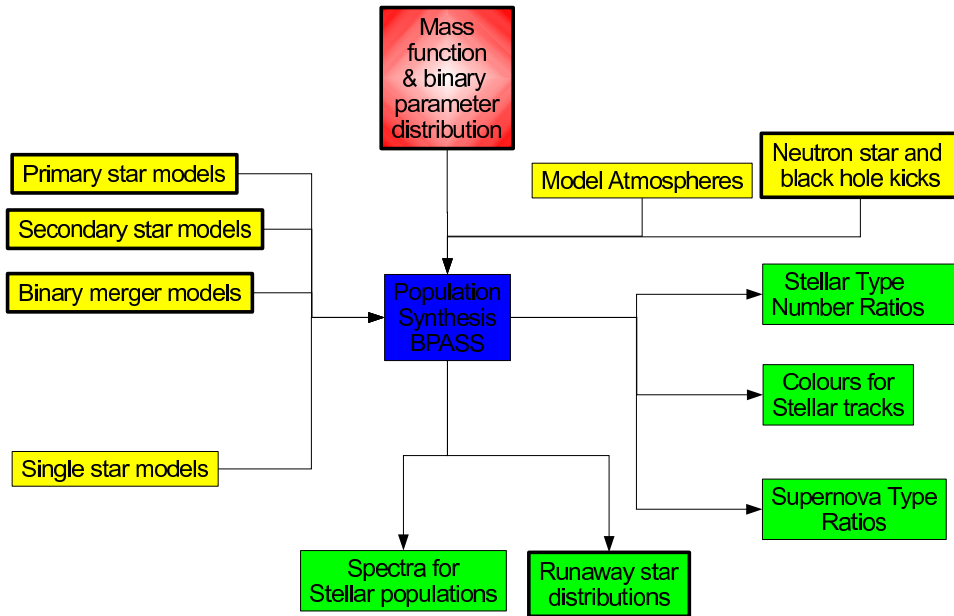


Figure 1. Schematic diagram showing the inputs and outputs of population synthesis codes. The boxes with thick borders indicate those unique to BPASS.

2. Numerical Method

Recently we have developed a novel and unique code to produce synthetic stellar populations that include binary stars (Eldridge & Stanway 2009). Figure 1 illustrates the inputs and outputs that make this code unique. For example the binary models that also require other new details such as the initial binary parameter distribution and the effect of neutron star and black hole kicks to determine the fate of the binaries after the first supernova. We also obtain extra predicted outputs such as the velocity distribution of runaway stars.

While similar codes exist, for example Leitherer et al. (1999), Kotulla et al. (2009) and Vanbeveren et al. (2007). BPASS has four important features each of which set it apart from other codes and in combination make it the state-of-the-art. First, and most important, is the inclusion of binary evolution in modelling the stellar populations. The general effect of binaries is to cause a population of stars to look bluer at older ages than predicted by single-star models. Second is that detailed stellar evolution models are used rather than an approximate rapid population synthesis method. Third is the use of only theoretical model spectra in our synthesis with as few empirical inputs as possible to create a completely synthetic model to compare with observations. Finally, the use of CLOUDY (Ferland et al. 1998) to determine the nebular emission means we are modelling not only the stars in detail but also the surrounding gas.

To provide an example of the importance of binaries in stellar populations we show in Figure 2 how a binary stellar population provides a similar spectrum to that of a single stellar population with a shallow IMF of -1.35 (where Salpeter IMF is -2.35). We see that the differences between a shallow IMF and binary evolution are small, on the order of 10%. The difference between them to the normal Salpeter single star

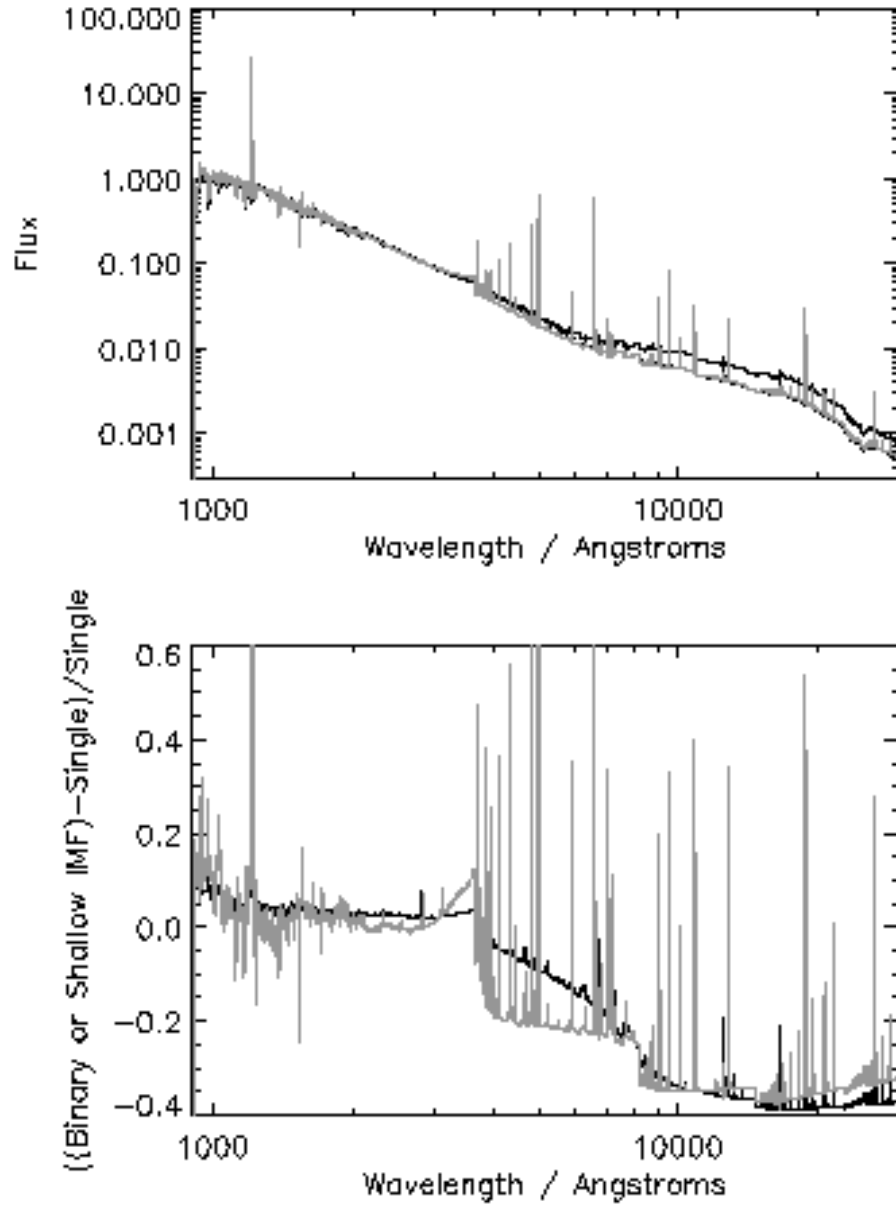


Figure 2. Upper panel: the spectra of single star (solid black lines), binary (grey line) and shallow IMF (dashed black line) populations. The greatest difference is at longer wavelengths. Lower panel: fractional difference between single star spectrum and those of a single star population with shallow IMF (solid black line) and binary population (solid grey line).

spectrum is up to 40%. The main identifying feature of the binary spectrum is that the spectrum has more ionizing flux. This leads to the spectral shape being dominated by the steps of the nebular continuum emission and the very strong nebular emission lines, which may provide a method to distinguish if we are observing a varying IMF or a binary dominated population.

BPASS and its comparison to various observations are discussed in detail in Eldridge et al. (2008) and Eldridge & Stanway (2009). Some results are available for download at <http://www.bpass.org.uk>. The code is versatile and adaptable to answer any question that requires knowledge of stellar populations. Here we have altered the code to take account of the stochastic nature of the filling of the IMF. We have created multiple realisations of clusters and galaxies populating the stellar and cluster IMFs at random rather than assuming a smooth IMF or star-formation history. With the code we have tested two schemes of filling the IMF. First, a *pure stochastic sampling* (PSS), where it is possible to have a $100M_{\odot}$ star in a $100M_{\odot}$ cluster (although it is very unlikely). The second scheme is that the maximum mass of a star, M_{\max} , in a cluster, of mass M_{cl} , is dependent on the total cluster mass. We calculate the maximum star mass from

$$\log(M_{\max}/M_{\odot}) = 2.56 \log(M_{\text{cl}}/M_{\odot}) (3.82^{9.17} + (\log(M_{\text{cl}}/M_{\odot}))^{9.17})^{\frac{-1}{9.17}} - 0.38, \quad (1)$$

which was derived by Pflamm-Altenburg et al. (2007). In this scheme in a $100M_{\odot}$ cluster the maximum stellar mass is $9.1M_{\odot}$. We refer to this as the *variable maximum mass* (VMM) case. In both cases we limit the most massive stars to $120M_{\odot}$.

We create the stellar population of a synthetic cluster by first setting the maximum stellar mass in the cluster from one of the two methods above. I.e. $120M_{\odot}$ in the PSS case or from the above equation in the VMM case. Then we pick the masses of stars in the cluster at random from the IMF. We use a Salpeter slope of -2.35 above $0.5M_{\odot}$ and -1.3 below this mass to $0.1M_{\odot}$. We continue to pick stars until the total mass of the stars is greater than our target cluster mass. When the last star is added to the cluster we examine the difference between the final and target cluster mass, whether the difference is smaller with or without the last star. We use the case with the smallest difference.

The situation for binary populations is slightly more complicated. When we consider a binary population we assume that each star above $5M_{\odot}$ has a binary companion and at random give the star a mass ratio and separation. The mass ratio distribution is flat over the range $0 < M_2/M_1 < 1$ and a separation distribution is flat in $\log a$ over the range of separations from 10 to $10^4 R_{\odot}$. We include the mass of the secondary companion in the total mass of the stellar population.

This is the case for a single cluster and can be repeated many times to understand the range of possible clusters. We use many synthetic clusters in Section 3.1 below. When we simulate the stellar population of an entire galaxy we do so by forming multiple stellar clusters with masses determined from a cluster mass function. The probability of a cluster mass is, $P(M_{\text{cl}}) \propto M_{\text{cl}}^{-2}$. We take the minimum cluster mass to be $50M_{\odot}$ and a maximum cluster mass of $10^6 M_{\odot}$. A key difference in our method to other such simulations is that rather than fixing the star-formation history to some smooth function we give each cluster a random age from over 100 Myrs. We then continue to create synthetic clusters until the total mass of stars in the galaxy averaged over 100 Myrs gives the required star-formation rate. For example to achieve a mean star formation rate of $1M_{\odot}/\text{yr}$ requires $10^8 M_{\odot}$ of stars. We find that the random star-formation history produces a greater scatter into our predicted observables as seen below. Our reasoning

behind this is that nature forms clusters as distinct components and there is no reason to expect different clusters to all form at the same time.

Once we have our synthetic stellar populations of either single clusters with a single age or a collection of clusters with a range of ages we can predict various required observables. Here we concentrate on two, the $H\alpha$ and UV fluxes that are both used as SFRs. $H\alpha$ is provided by stars more massive than $20M_{\odot}$, while UV flux is produced by stars down to $3M_{\odot}$. Examining these two indicators we have some idea regarding how the upper end of the IMF is populated and which of PSS or VMM is in action in the Universe.

3. Results

Theoretical models are limited in their use without comparison to observations. Comparison both checks the model accuracy and enables us to learn something about the physics in action in the Universe. Here we compare our synthetic populations to observations of individual star clusters and the emission from nearby galaxies.

3.1. Individual Clusters

Recently Calzetti et al. (2010) have attempted to measure the $H\alpha$ emission from a number of young stellar clusters to determine the mean $H\alpha$ emission per Solar mass of material in a cluster. A number of clusters have been observed in $H\alpha$ that are selected to have ages between 1 to 8Myrs from their broad-band colours. In Calzetti et al. (2010) the sample of clusters are then binned into two mass ranges. The idea behind this is that if the sampling of the IMF is by PSS then a hundred $1000M_{\odot}$ clusters should have the same stellar population as one $10^5 M_{\odot}$ cluster. This means they should have the same $H\alpha$ flux per mass of stars. If there is a VMM then we should expect fewer massive star and therefore less $H\alpha$ per mass of stars. In Figure 3 we compare synthetic clusters to the observations of Calzetti et al. (2010). Making sure the models and observations have the same mass range and age range. We also include lines that represent the mean $H\alpha$ flux per mass for all the synthetic clusters in the mass range.

The single star $H\alpha$ flux decreases more rapidly with age than that for a binary population. Thus the single star population does have lower minimum $H\alpha$ fluxes, by about 0.4 dex after 8Myrs. When comparing to the observations there are two pairs of points from whether the clusters not detected in $H\alpha$ are included or not. It is apparent that the points in general agree more closely to PSS. Further evidence is supplied by the existence of the box in the Figures representing the Velorum cluster that has a total mass of 250 to $360M_{\odot}$. It includes two stars in a massive binary which have initial mass of 35 and $30M_{\odot}$. For such a cluster VMM predicts a maximum stellar mass of $19M_{\odot}$. While we cannot rule out there is a VMM this one example again points towards PSS being more likely.

3.2. 11HUGS Galaxies

Another consequence of varying the method of filling the IMF is that different SFRs based on different mass ranges of stars will give discrepant results at different galaxy-wide star-formation rates. Lee et al. (2009) estimated the SFR for a sample of galaxies from both their $H\alpha$ and UV fluxes. These results are shown in Figure 4 again compared to synthetic stellar populations. In this plot the synthetic galaxies assume constant star-

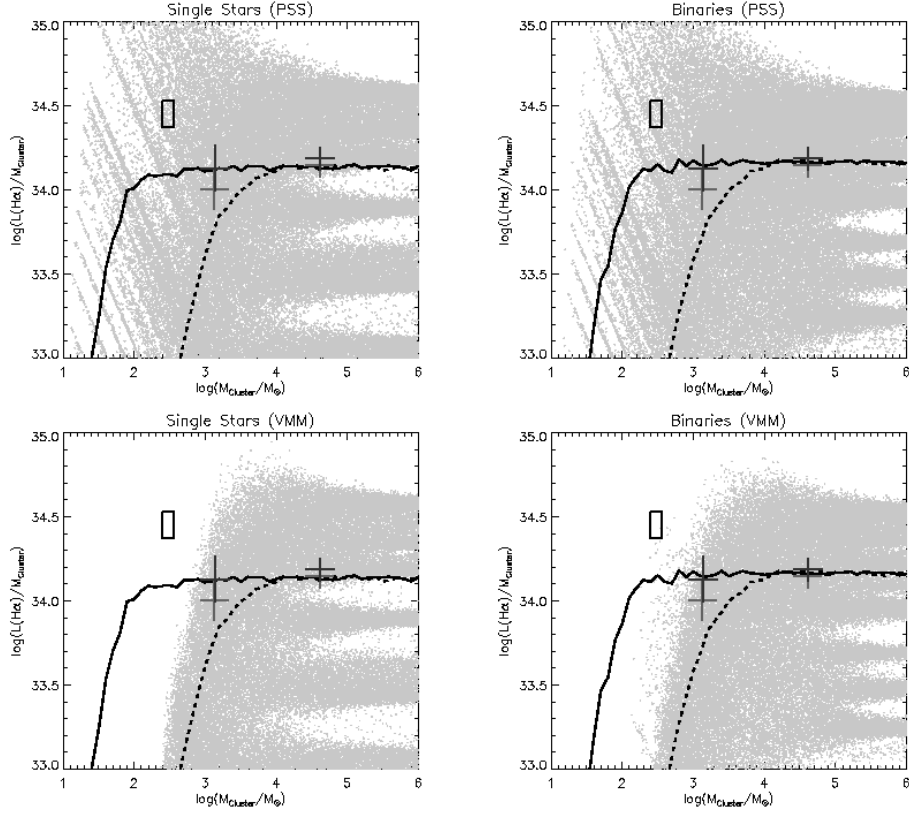


Figure 3. Plot of $H\alpha$ flux per stellar mass of material in clusters. The points are individual realisations of different clusters from two methods of filling the IMF: PSS for upper two panels and VMM for the lower two panels. The lines show the mean for these two methods, solid black line for PSS and dashed black line for VMM. The grey crosses represent the observations of Calzetti et al. (2010): light grey including clusters not detected in $H\alpha$ and dark grey not including them. The black box represents the values derived from the Velorum cluster estimated from Jeffries et al. (2009), De Marco et al. (2000) and Eldridge (2009). The left panels are for clusters including single stars and the right panels are for binary populations. The linear features in the points of the upper panels are due to the limited resolution of the stellar model's initial masses.

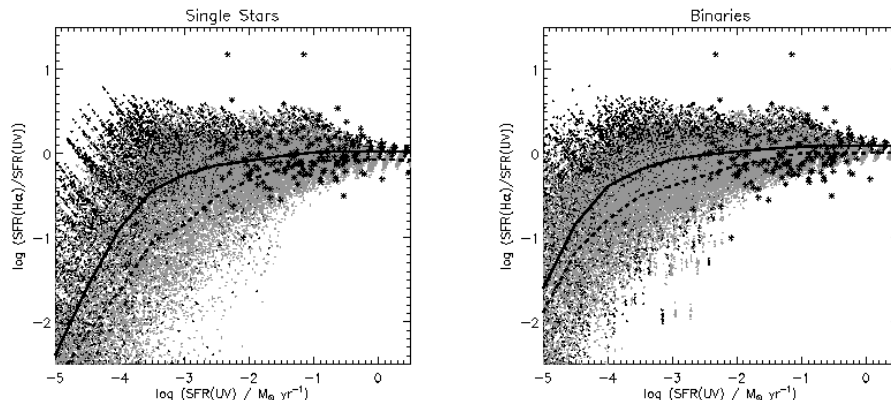


Figure 4. The ratio of SFR measured by $H\alpha$ and UV fluxes versus the SFR from UV flux. The asterisks are the observations from Lee et al. (2009) while the dots are individual realisations of synthetic galaxies. The lines indicate the mean ratios for PSS in the solid line and VMM for the dashed line. The left panel is for a single star population and the right panel for binary populations.

formation over a period of 100Myrs. The models predict that as the SFR decreases so to does the ratio of SFRs measured by $H\alpha$ and UV. This is because the $H\alpha$ flux is provided primarily by stars of over $20M_{\odot}$ while stars down to $3M_{\odot}$ provide UV flux. At low SFRs it becomes less likely to get the massive stars required but all less likely for them to be formed recently enough to contribute to the $H\alpha$ emission.

It has been suggested by Pflamm-Altenburg et al. (2009) that the turn down of this ratio as evidence for a VMM. However here we show that much of the observed scatter can be explained by a stochastic star-formation history. Furthermore this ratio is only an upper limit to the expected ratio. There is growing evidence that the covering factor of young HII regions is less than unity and therefore many ionizing photons might escape galaxies and not produce $H\alpha$ emission. The UV flux is a direct measure of the flux from the stars themselves so is a more reliable measure of the actual mass of stars present.

In Figure 4 if the single star and binary populations are compared we see that there is little difference in the range of scatter. The binary population ratio however does not decrease as rapidly as the single star populations. This is because the effect of binaries is to increase the number of hot and luminous stars and therefore provide more $H\alpha$ over a longer timescale. Again we should not expect such a rapid turn down as suggested by Pflamm-Altenburg et al. (2009).

Further work is required in simulating these galaxies but we see here that to determine how the IMF is filled cannot be measured from the $H\alpha$ to UV ratio unless a large number of very low star-formation rate galaxies are observed.

4. Conclusions

In population synthesis the IMF is an uncertain factor, so to is the evolution of stars. Many of the results that are used to infer that the IMF is variable may be explained away when binaries are included in population synthesis.

The $H\alpha$ flux per Solar mass observed in samples of clusters agrees with PSS of the IMF. However more observations are required to rule out a VMM. Individual low-mass clusters with one or two massive OB and WR stars are perhaps the most strict test to distinguish between PSS and VMM and therefore more such clusters should be searched for.

The ratio of the $H\alpha$ and UV flux SFRs in galaxies has a significant scatter that can be explained by the stochastic nature of the star-formation history, rather than IMF variations or a VMM. The ratio of SFRIs for stellar populations including binaries varies less than that for populations of single star models only. This is because binaries can experience mergers and mass-transfer and produce more massive stars. However finding the low-star-formation rate galaxies required to decide between PSS and VMM is difficult. Also measuring the SFRIs accurately in such galaxies is difficult. Using a wider range of SFRIs and observables beyond those presented here is a more promising avenue to take to discriminate between PSS and VMM. This requires further development of BPASS to include more physical processes in greater detail.

Acknowledgments. JJE would like to thank Benjamin Johnson, Monica Relano, Dan Weisz, Daniella Calzetti, Janice Lee and Rob Kennicutt for useful discussion. He is supported by the Theory Rolling Grant at the Institute of Astronomy, University of Cambridge.

References

- Calzetti, D., Chandar, R., Lee, J. C., Elmegreen, B. G., Kennicutt, R. C., & Whitmore, B. 2010, ArXiv e-prints. 1007.3188
- De Marco, O., Schmutz, W., Crowther, P. A., Hillier, D. J., Dessart, L., de Koter, A., & Schweickhardt, J. 2000, A&A, 358, 187. arXiv:astro-ph/0004081
- Eldridge, J. J. 2009, MNRAS, 400, L20. 0909.0504
- Eldridge, J. J., Izzard, R. G., & Tout, C. A. 2008, MNRAS, 384, 1109. 0711.3079
- Eldridge, J. J., & Stanway, E. R. 2009, MNRAS, 400, 1019. 0908.1386
- Ferland, G. J., Korista, K. T., Verner, D. A., Ferguson, J. W., Kingdon, J. B., & Verner, E. M. 1998, PASP, 110, 761
- Jeffries, R. D., Naylor, T., Walter, F. M., Pozzo, M. P., & Devey, C. R. 2009, MNRAS, 393, 538. 0810.5320
- Kotulla, R., Fritze, U., Weilbacher, P., & Anders, P. 2009, MNRAS, 396, 462. 0903.0378
- Lee, J. C., Gil de Paz, A., Tremonti, C., Kennicutt, R. C., Salim, S., Bothwell, M., Calzetti, D., Dalcanton, J., Dale, D., Engelbracht, C., Funes, S. J. J. G., Johnson, B., Sakai, S., Skillman, E., van Zee, L., Walter, F., & Weisz, D. 2009, ApJ, 706, 599. 0909.5205
- Leitherer, C., Schaerer, D., Goldader, J. D., González Delgado, R. M., Robert, C., Kune, D. F., de Mello, D. F., Devost, D., & Heckman, T. M. 1999, ApJS, 123, 3. arXiv:astro-ph/9902334
- Pflamm-Altenburg, J., Weidner, C., & Kroupa, P. 2007, ApJ, 671, 1550. 0705.3177
- 2009, MNRAS, 395, 394. 0901.4335
- Vanbeveren, D., Van Bever, J., & Belkus, H. 2007, ApJ, 662, L107. arXiv:astro-ph/0703796